Single phosphorylation sites in Acc1 and Acc2 regulate lipid homeostasis and the insulin–sensitizing effects of metformin

Morgan D. Fullerton[†], Sandra Galic[†], Katarina Marcinko, Sarah Sikkema, Thomas Pulinilkunnil, Zhi–Ping Chen, Hayley M. O'Neill, Rebecca J. Ford, Rengasamy Palanivel, Matthew O'Brien, D. Grahame Hardie, S. Lance Macaulay, Jonathan D. Schertzer, Jason R. B. Dyck, Bryce J. van Denderen, Bruce E. Kemp, Gregory R. Steinberg[*]

Supplementary Figure 1

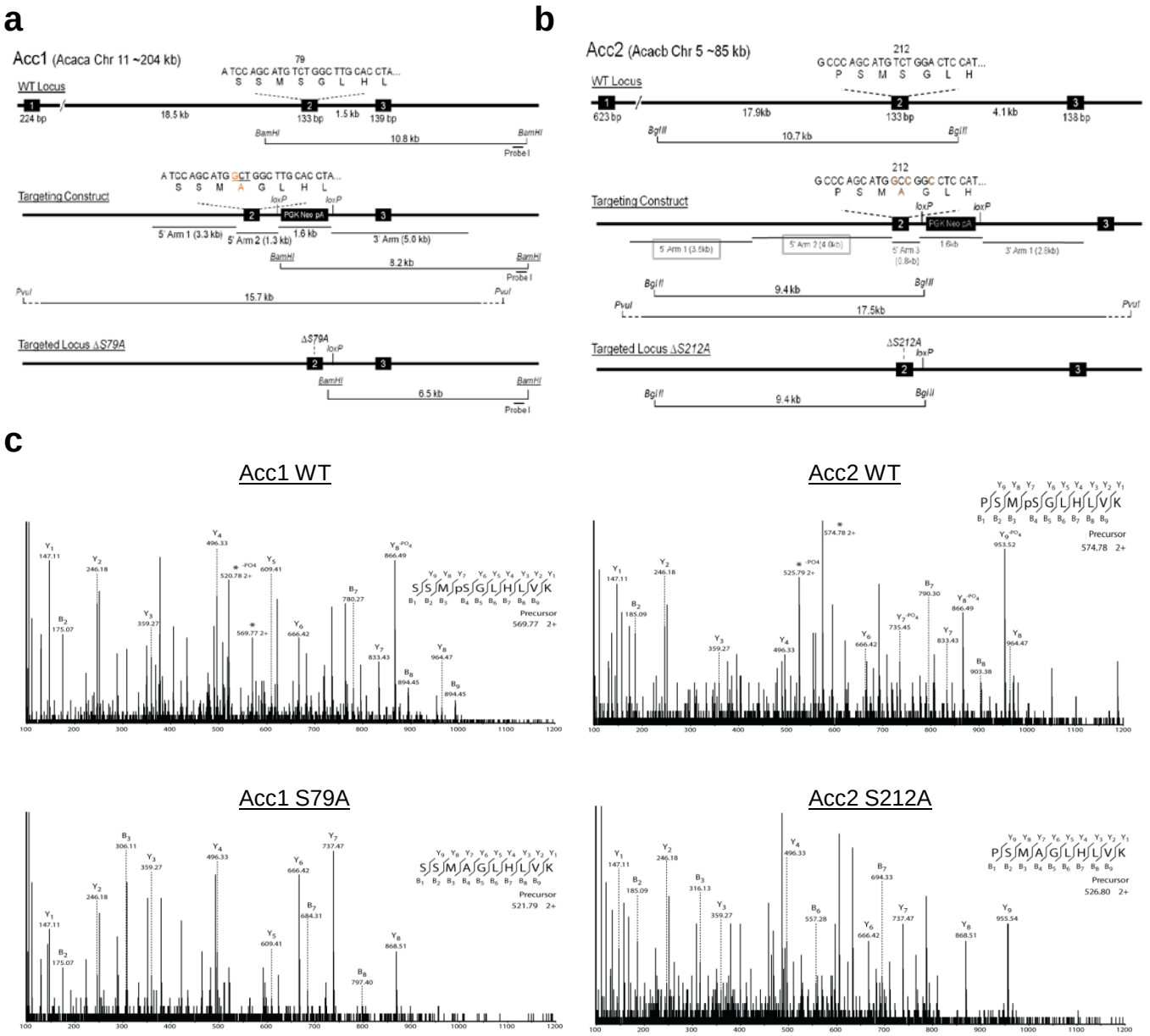

Supplementary Fig. 1. Generation and confirmation of Acc1KI and Acc2KI mice. Schematic representation of the targeting strategy for (**a**) Acc1KI and (**b**) Acc2KI mice. (**c**) Summary of mass spectroscopy analyses of the Ser–Ala mutation on Acc1 and Acc2, where the precursor denotes the charge at the site of the mutation at Acc1 Ser79 and Acc2 Ser212.

Supplementary Figure 2

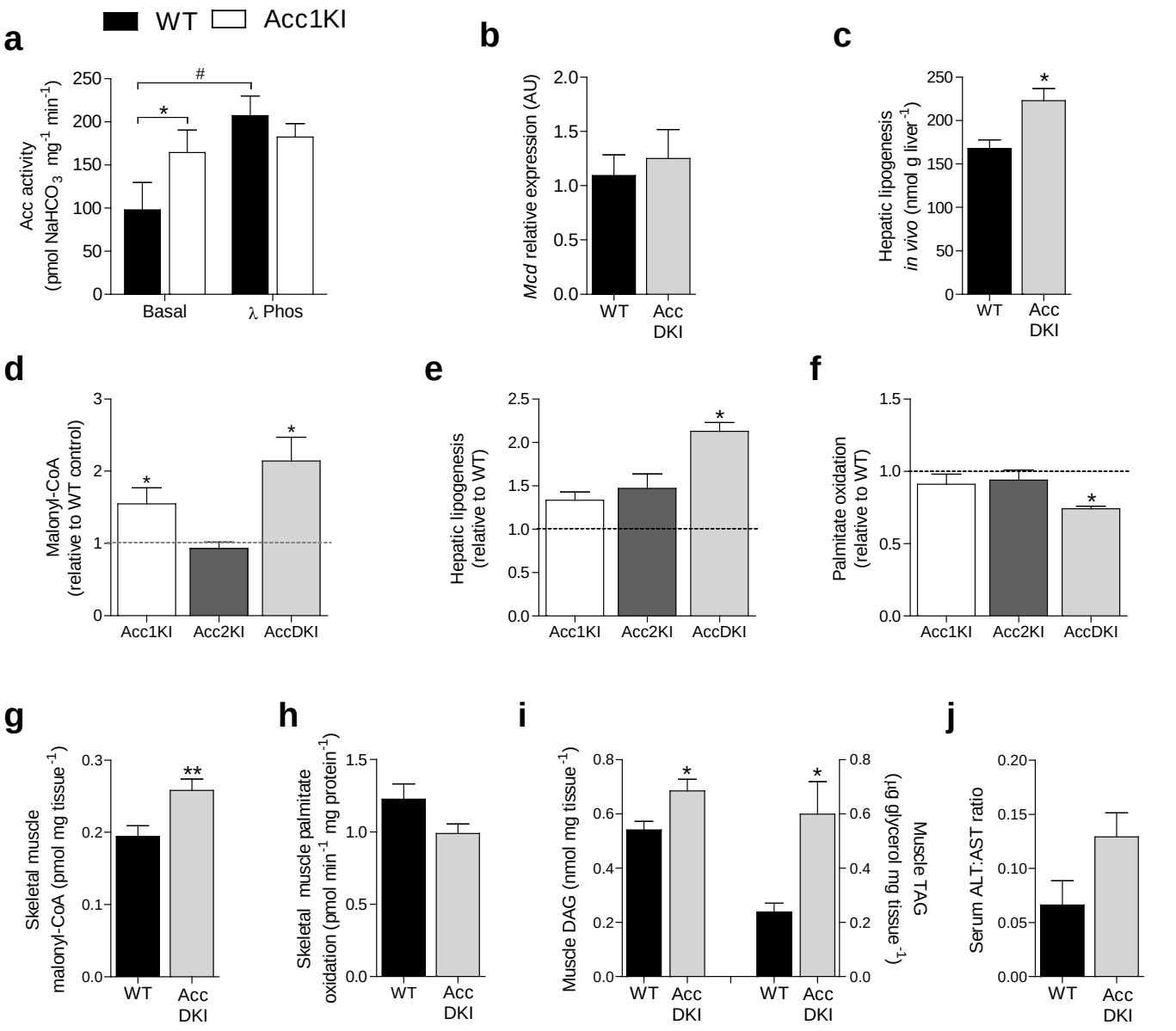

Supplementary Fig. 2. Metabolic profile of Acc1KI, Acc2KI and AccDKI in liver and skeletal muscle. (**a**) Acc1 enzyme activity was assessed under basal conditions (in the absence of citrate) and after λ phosphatase treatment from WT and Acc1KI livers (n = 4). (**b**) Liver malonyl–CoA decarboxylase (*Mcd*) expression in AccDKI mice relative to WT control (n = 7–8). (**c**) The *in vivo* incorporation of [^{3}H]–acetate into total liver lipid as a measure of *de novo* lipogenesis (n = 5). (**d**) Liver malonyl–CoA levels (n = 7–8), (**e**) hepatocyte lipogenesis ([^{3}H]–acetate incorporation into TAG) and (**f**) hepatocyte [^{14}C]–palmitate oxidation from Acc1KI, Acc2KI and AccDKI mice, expressed relative to WT control (n = 3 from at least 3 separate experiments). (**g**) Skeletal muscle malonyl–CoA in the fed–state (n = 8). (**h**) [^{14}C]–Palmitate oxidation in isolated *extensor digitorum longus* muscle (n = 8–10). (**i**) Skeletal muscle DAG and TAG (n = 6–8). (**j**) The serum activities of markers of liver function, alanine aminotransferase (ALT) as a ratio of aspartate aminotransferase (AST) between WT control and AccDKI (n = 7–8). Data are expressed as means ± SEM, where * $P < 0.05$ and ** $P < 0.01$ compared to WT control, $^{\#}$ $P < 0.05$ compared to basal treatment as determined by Student's t test or an ANOVA and Bonferonni *post hoc* test, respectively. *Mcd* relative gene expression was normalized to *Actb*.

Supplementary Figure 3

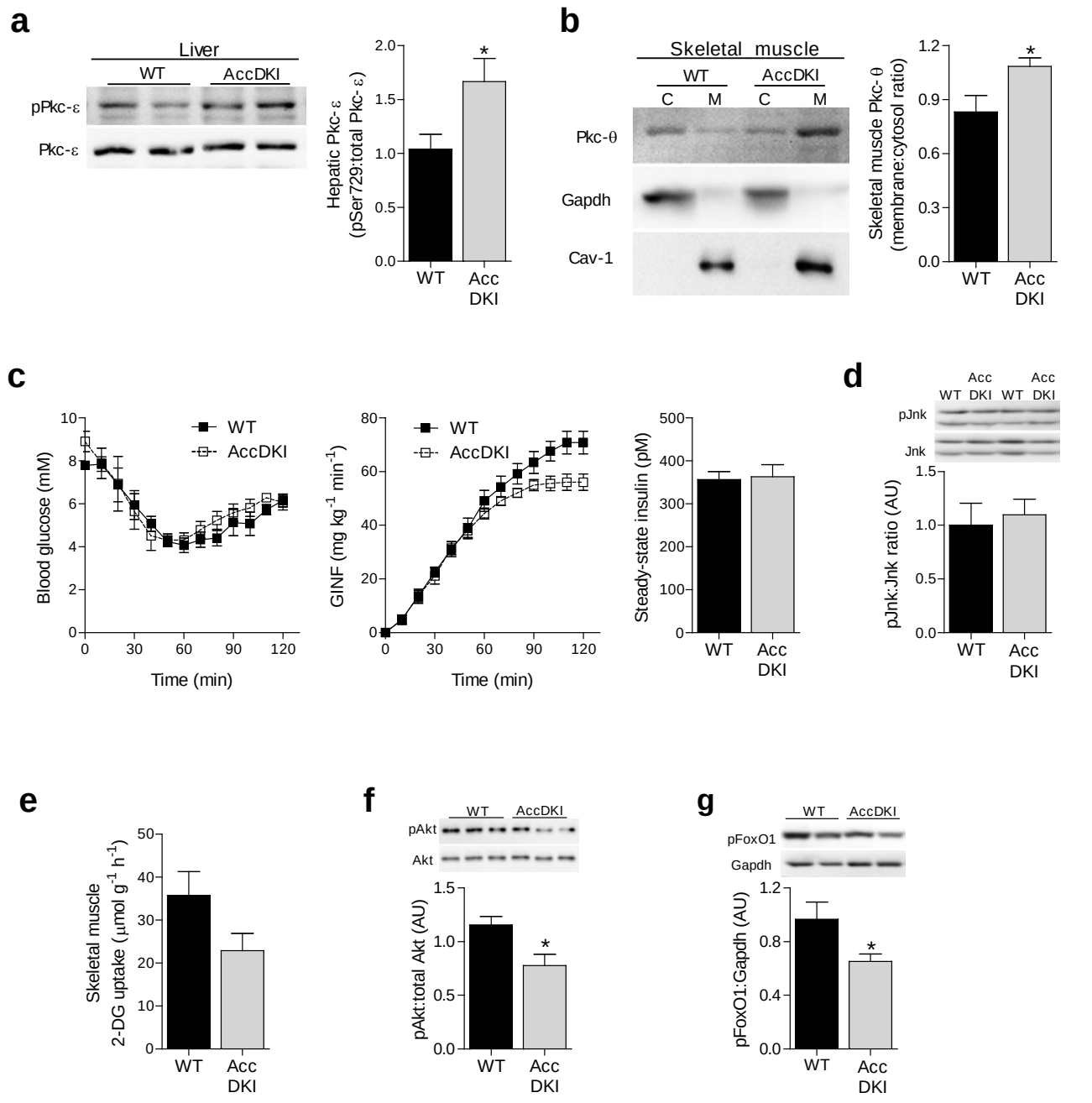

Supplementary Fig. 3. Lipid parameters, Pkc activation and insulin sensitivity in chow mice. (**a**) Liver Pkc–ε Ser729 phosphorylation (n = 7). (**b**) Skeletal muscle membrane–associated Pkc–θ (n = 7), shown as the ratio of membrane:cytosolic fraction. (**c**) Blood glucose measurements and glucose infusion rates (GINF) over the time course of the clamp procedure, as well as steady–state insulin levels at the termination of the clamp for chow–fed mice (n = 7–8). (**d**) Representative blot and densitometry showing phosphorylation of liver Jnk (n = 5). (**e**) [^{14}C]–2–deoxyglucose (2–DG) uptake into skeletal muscle during the clamp (n = 7–8), and skeletal muscle (**f**) Akt (Ser473) phosphorylation and (**g**) FoxO1 (Ser253) phosphorylation at the completion of the clamp (n = 7–8). Data are expressed as means ± SEM, where * P < 0.05 compared to WT control as determined by a Student's t test. Duplicate gels were run for quantification of total Akt and Jnk. For Pkc activation, Gapdh and caveolin–1 were used for cytosolic and membrane normalization, respectively, and blots shown are from duplicate gels.

Supplementary Figure 4

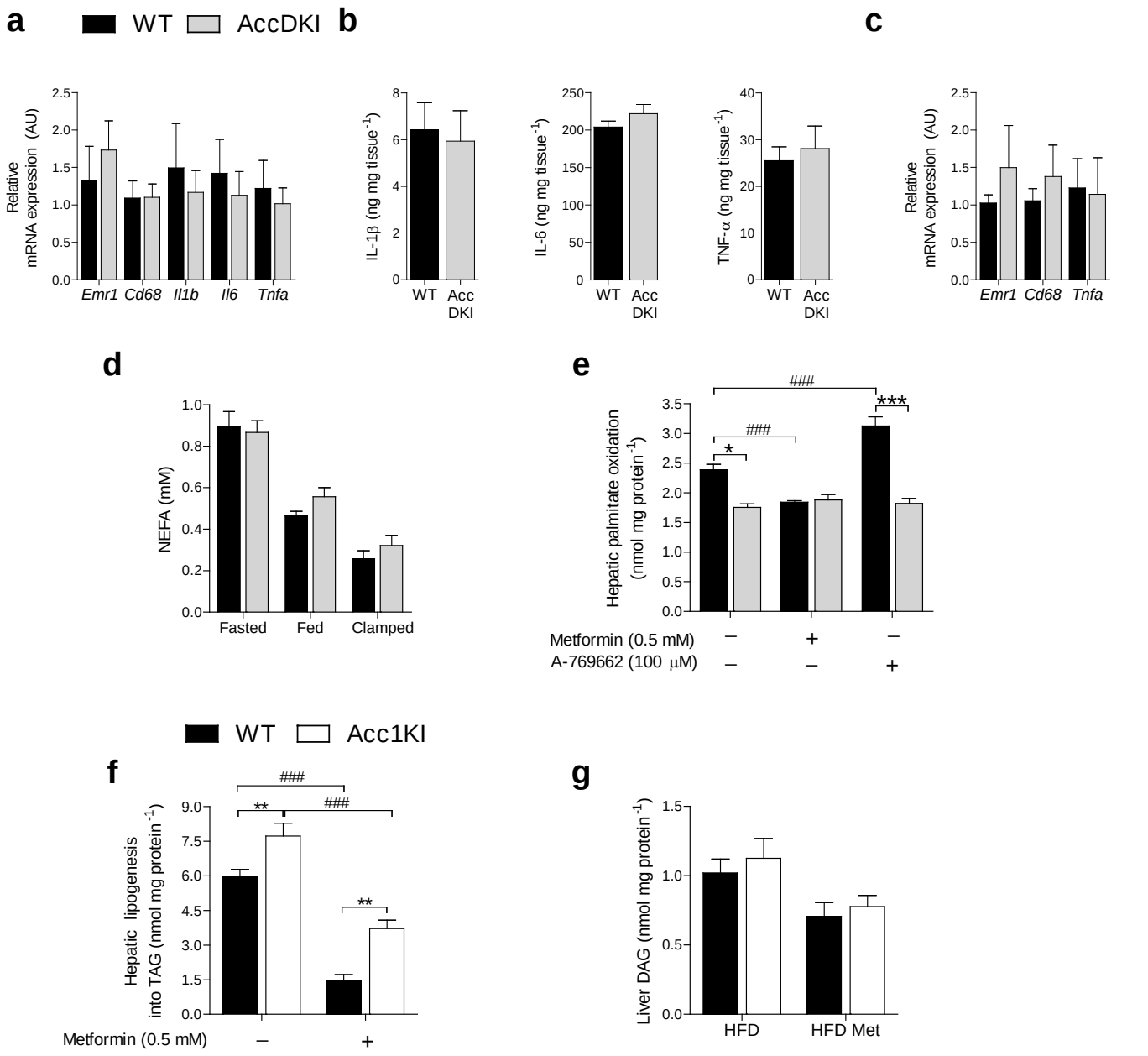

Supplementary Fig. 4. AccDKI insulin resistance is not due to inflammation or higher serum fatty acids, and metformin requires Acc1 and Acc2 phosphorylation. (**a**) The relative expression of macrophage–specific transcripts as well as pro–inflammatory cytokines in the liver (n = 7–8). (**b**) Hepatic pro–inflammatory cytokine protein levels IL–1β, IL–6 and TNF–α (n = 8). (**c**) The relative expression of macrophage–specific transcripts as well as pro–inflammatory cytokines in the epididymal white adipose tissue (WAT) (n = 7–8). (**d**) Circulating non–esterified fatty acids (NEFA) in the fasted–, fed– and clamped–state (n = 7–16). (**e**) [^{14}C]–palmitate oxidation from WT and AccDKI hepatocytes (n = 3–4 from at least 2 separate experiments). (**f**) [^{3}H]–acetate incorporation into TAG was measured from WT and Acc1KI hepatocytes (n = 3 from 2 separate experiments). (**g**) Hepatic DAG from HFD–fed WT and Acc1KI mice chronically treated with 50 mg/kg metformin (n = 8–12). Data are expressed as mean ± SEM, * $P < 0.05$, ** $P < 0.01$ and *** $P < 0.001$ compared to WT and $^{###}$ $P < 0.001$ compared to vehicle control as determined by ANOVA and Bonferonni *post hoc* test, and relative gene expression was normalized to *Actb*.

Supplementary Figure 5

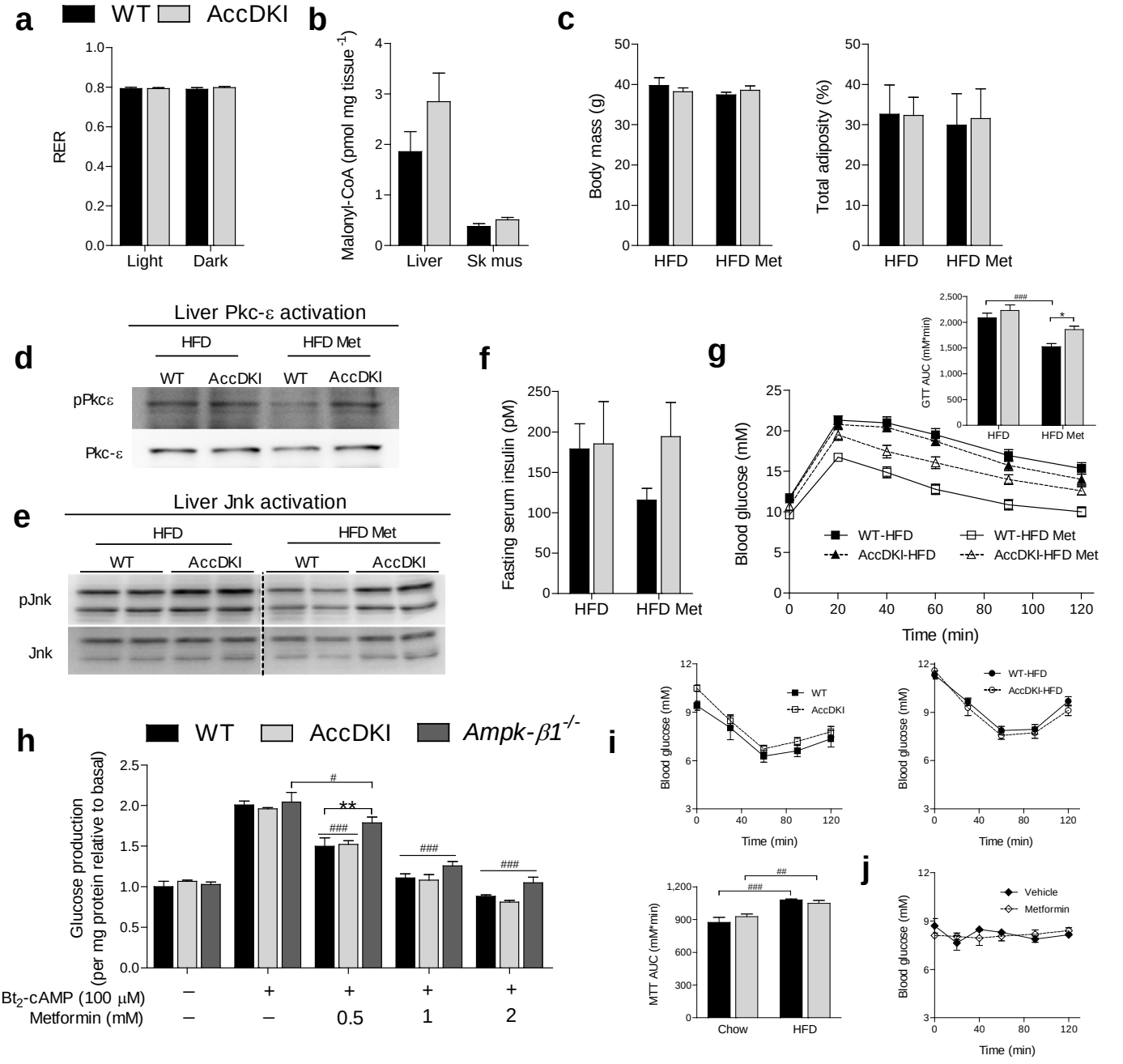

Supplementary Fig. 5. Lipid metabolism is normalized in AccDKI HFD mice and the acute effects of metformin to suppress hepatic glucose are independent of Acc phosphorylation. (**a**) Respiratory exchange ratio (RER) from HFD-fed WT and AccDKI mice. (**b**) Liver and skeletal muscle malonyl–CoA from HFD–fed WT and AccDKI mice in the fed–state (n = 8). (**c**) Final body mass and percent adiposity (n = 10). (**d**) Phosphorylated Pkc–ε (Ser729) and (**e**) phosphorylation of Jnk in the liver of HFD and HFD–metformin treated mice (n = 7). (**f**) Fasting serum insulin levels and (**g**) glucose tolerance test (1 g/kg) and area under the curve (n = 10). (**h**) Glucose production in primary hepatocytes treated with or without increasing concentrations of metformin (n = 5 from at least 2 separate experiments). (**i**) Metformin tolerance test (200 mg/kg) in overnight–fasted WT and AccDKI mice fed a regular chow diet (n = 5), or a HFD (n = 7–8), with associated area under the curve. (**j**) Metformin tolerance test (50 mg/kg or saline vehicle) in overnight–fasted WT mice fed a regular chow diet (n = 5). Data are expressed as mean ± SEM, for area under the curve, * P < 0.05 compared to WT and $^{\#\#}$ P < 0.01 and $^{\#\#\#}$ P < 0.001 compared to control diet. For hepatocytes, ** P < 0.01 compared to WT and $^{\#}$ P < 0.05 and $^{\#\#\#}$ P < 0.001 compared to no Bt_2–cAMP control as determined by ANOVA and Bonferonni *post hoc* test. Duplicate gels were run for quantification of total Pkc–ε and Jnk.

Supplementary Figure 6

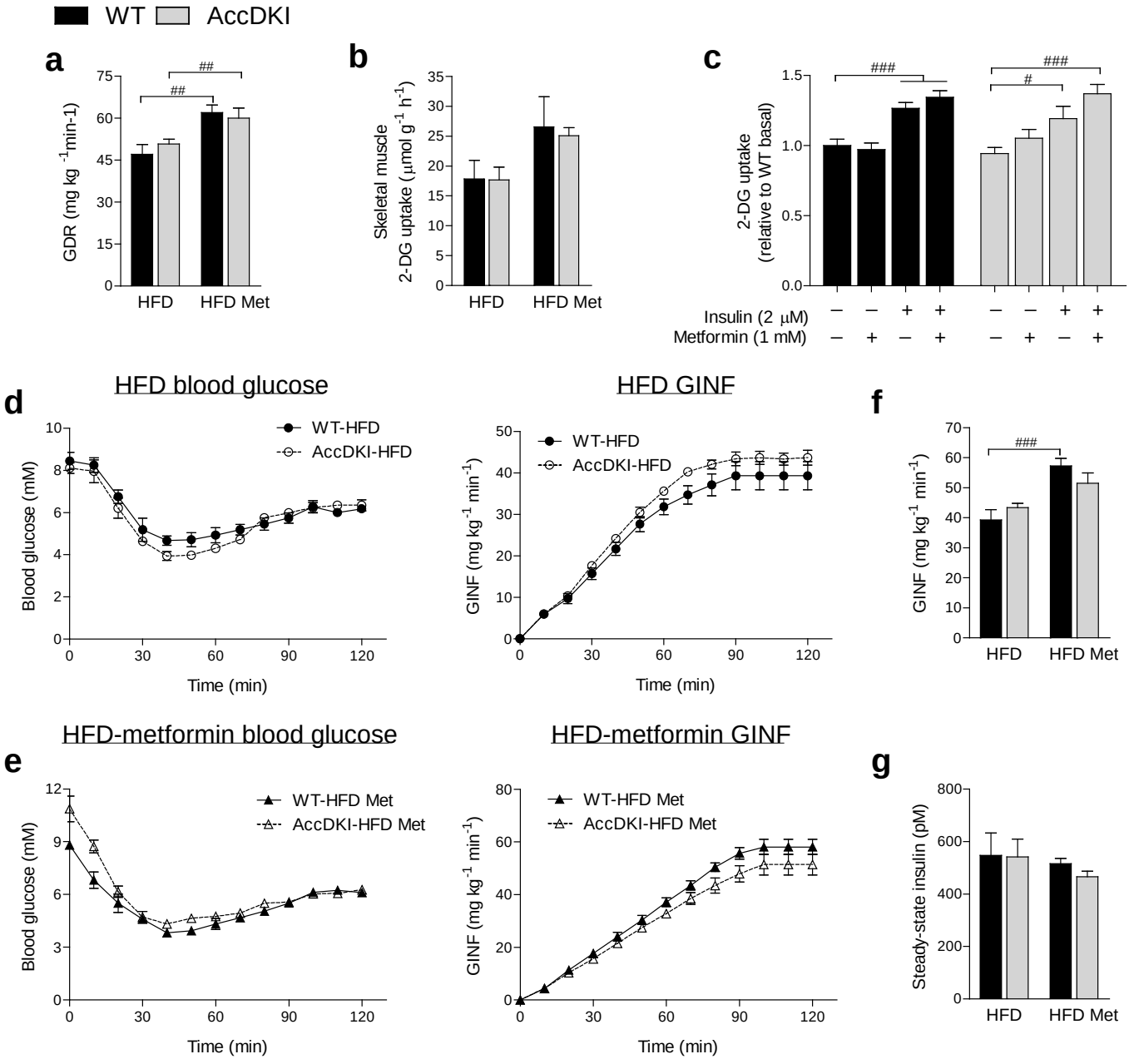

Supplementary Fig. 6. Chronic metformin treatment increases skeletal muscle glucose uptake independent of Acc phosphorylation. (**a**) Glucose disposal rate (GDR) for HFD–control and HFD–metformin treated WT and AccDKI mice (n = 7–8). (**b**) [^{14}C]–2–deoxyglucose (2–DG) uptake into skeletal muscle during the clamp (n = 7–8). (**c**) [^{3}H]–2–DG uptake in isolated *ex vivo* stimulated *extensor digitorum longus* muscle from WT or AccDKI mice (n = 5–6). Hyperinsulinemic–euglycemic clamp results for blood glucose measurements and glucose infusion rate (GINF) over the time course of the clamp procedure for (**d**) HFD control, (**e**) HFD–metformin treated WT and AccDKI mice and (**f**) a summary of final rates (n = 7–8). (**g**) Steady–state insulin levels at the termination of the clamp (n = 7–8). Data are expressed as mean ± SEM, $^{\#}$ $P < 0.05$, $^{\#\#}$ $P < 0.01$ and $^{\#\#\#}$ $P < 0.001$ compared to control treatment as determined by ANOVA and Bonferonni *post hoc* test.

Supplementary Figure 7

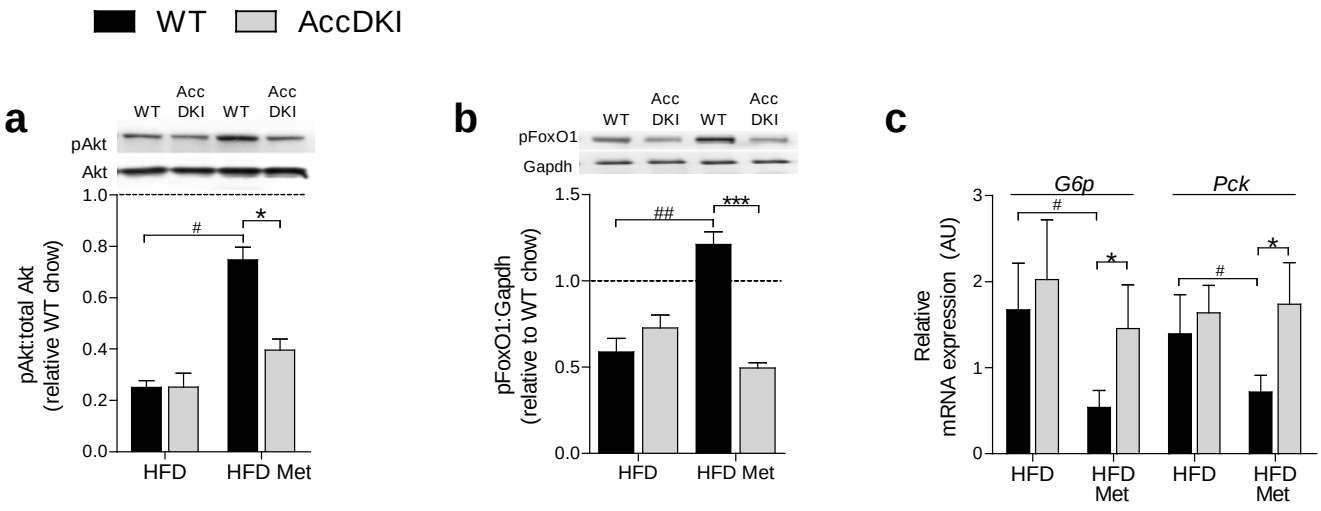

Supplementary Fig. 7. Chronic metformin treatment improves hepatic insulin action in WT mice, but not AccDKI. (**a**) Liver Akt (Ser473) phosphorylation, (**b**) liver FoxO1 (Ser253) phosphorylation shown relative to chow WT control (n = 5) and (**c**) gluconeogenic gene expression (*G6p* and *Pck*) at the completion of the clamp (n = 8). Data are expressed as means ± SEM, * $P < 0.05$ and *** $P < 0.001$ represent differences between genotype, and $^{\#}P < 0.05$ and $^{\#\#}P < 0.01$ are differences between treatment as determined by ANOVA and Bonferonni *post hoc* test. Relative gene expression was normalized to *Actb* and duplicate gels were run for quantification of total Akt and Gapdh.

Supplementary Figure 8

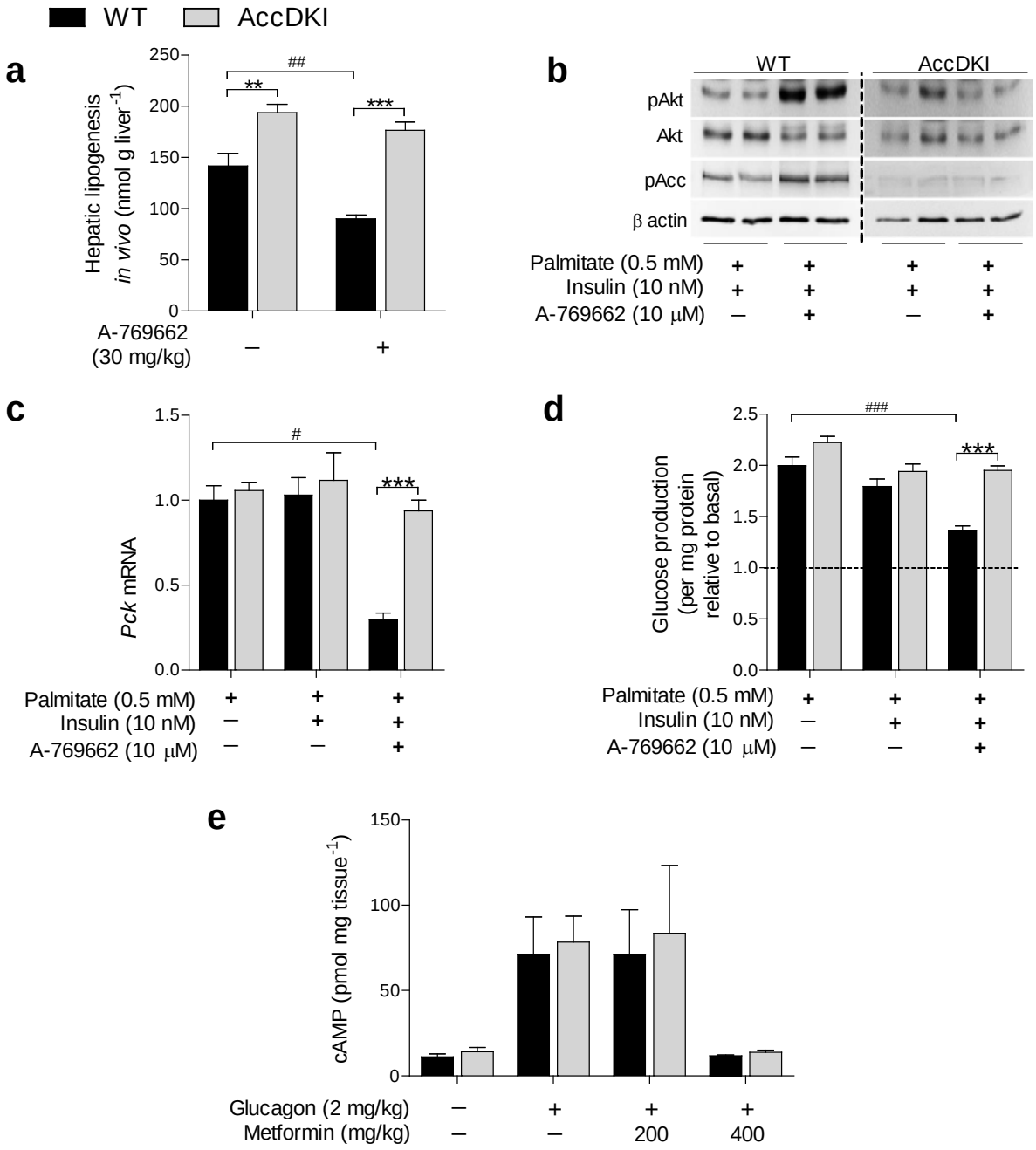

Supplementary Fig 8. Specific Ampk activation requires Acc signaling, but metformin–induced suppression of glucagon-stimulated cAMP does not. (**a**) *In vivo* incorporation of [^{3}H]–acetate into total liver lipid (*de novo* lipogenesis) in WT and AccDKI mice treated with vehicle (5% DMSO in PBS) or A–769662 (30 mg/kg) (n = 4 for vehicle and n = 5 for A–769662). Primary hepatocytes were treated ± A–769662 (10 μM) in the presence of palmitate (0.5 mM) for 18 h and insulin (10 nM) stimulation of (**b**) Akt (Ser473) phosphorylation or suppression of (**c**) *Pck* expression determined (shown relative to WT, palmitate control) (n = 2–4). (**d**) Insulin suppression of hepatic glucose production, following chronic (18 h) exposure to palmitate (0.5 mM) ± A–769662 (10 μM) (n = 3–4, from at least 2 separate experiments). Hatched line represents no Bt_2–cAMP. (**e**) Hepatic glucagon–stimulated cAMP in WT and AccDKI mice administered vehicle (saline), 200 or 400 mg/kg metformin in the fed–state were (n = 3–4). Data are expressed as means ± SEM, ** $P < 0.01$ and *** $P < 0.001$ represent differences between genotype, and $^{\#}P < 0.05$, $^{\#\#}P < 0.01$ and $^{\#\#\#}P < 0.001$ are differences between treatment, as determined by ANOVA and Bonferonni *post hoc* test. Duplicate gels were run for total Akt and β actin, where all samples from both genotypes were run on the same gel, but WT and DKI samples were imaged separately.